Brief Report

Effect of M694V mutation in the MEFV gene, associated with Familial Mediterranean fever, on the morphology of iPSC-derived macrophages

Elena V. Grigor'eva , Lana V. Karapetyan , Anastasia A. Malakhova , Sergey P. Medvedev , Julia M. Minina , Varduhi H. Hayrapetyan , Valentina S. Vardanyan , Suren M. Zakian , Arsen Arakelyan , Roksana Zakharyan *

Posted Date: 20 March 2024

doi: 10.20944/preprints202403.1184.v1

Keywords: Familial Mediterranean fever; macrophages; patient-specific induced pluripotent stem cells; differentiation; MEFV gene

Brief Report

Effect of M694V Mutation in the *MEFV* Gene, Associated with Familial Mediterranean Fever and on the Morphology of iPSC-Derived Macrophages

Elena V. Grigor'eva [1,2,3], Lana V. Karapetyan [4], Anastasia A. Malakhova [1,2,3], Sergey P. Medvedev [1,2,3], Julia M. Minina [1], Varduhi H. Hayrapetyan [4,5], Valentina S. Vardanyan [6,7], Suren M. Zakian [1,2,3], Arsen Arakelyan [4,5] and Roksana Zakharyan [4,5,*]

1 Institute of Cytology and Genetics, Siberian Branch of Russian Academy of Sciences, Novosibirsk, Russia; evlena@bionet.nsc.ru; amal@bionet.nsc.ru; medvedev@bionet.nsc.ru; minina_jul@bionet.nsc.ru; zakian@bionet.nsc.ru
2 Meshalkin National Medical Research Center, Ministry of Health of the Russian Federation, 630055 Novosibirsk, Russia; evlena@bionet.nsc.ru; amal@bionet.nsc.ru; medvedev@bionet.nsc.ru; zakian@bionet.nsc.ru
3 Institute of Chemical Biology and Fundamental Medicine, Siberian Branch of Russian Academy of Sciences, 630090 Novosibirsk, Russia; evlena@bionet.nsc.ru; amal@bionet.nsc.ru; medvedev@bionet.nsc.ru; zakian@bionet.nsc.ru
4 Russian-Armenian (Slavonic) University, Yerevan, Armenia; lana.karapetyan@rau.am; arsen.arakelyan@rau.am; roksana.zakharyan@rau.am; varduhi.hairapetyan@rau.am
5 Institute of Molecular Biology NAS RA, Yerevan, Armenia; varduhi.hairapetyan@rau.am; aarakelyan@sci.am; roksana.zakharyan@rau.am
6 Associate Professor, Department of Rheumatology, Yerevan State Medical University (YSMU); valentina.vardanyan@gmail.com
7 Head of Rheumatology Department, "Mikaelyan" Institute of Surgery; valentina.vardanyan@gmail.com
* Correspondence: roksana.zakharyan@rau.am

Abstract: Familial Mediterranean fever (FMF) is a systemic autoinflammatory disorder caused by inherited mutations in the *MEFV* (Mediterranean FeVer) gene located on chromosome 16 (16p13.3) and coding pyrin protein. Despite the existing data on *MEFV* mutations, the exact mechanism of their effect on the development of pathological processes leading to autoinflammation observed in FMF, remains unclear. Induced pluripotent stem cells (iPSCs) are considered an important tool for studying the molecular genetic mechanisms of various diseases due to their ability to differentiate into any cell type, including macrophages, which contribute to the development of FMF. In this study, we developed iPSCs of an Armenian patient with FMF having M694V, p.(Met694Val) (c.2080A>G, rs61752717) pathogenic mutation in exon 10 of the *MEFV* gene. As a result of direct differentiation, macrophages expressing CD14 and CD45 surface markers were obtained. In addition, we found that the morphology of patient macrophages derived from iPSCs with *MEFV* mutation was significantly different from that of differentiated from iPSCs of a healthy donor carrying wild-type *MEFV* gene.

Keywords: Familial Mediterranean fever; macrophages; patient-specific induced pluripotent stem cells; differentiation; *MEFV* gene

1. Introduction

Familial Mediterranean fever (FMF) is a systemic autoinflammatory disorder characterized by recurrent episodes of fever and polyserositis (e.g. peritonitis, pleuritis, synovitis) symptoms. The FMF carrier frequencies are high in several eastern Mediterranean populations, ranging from 37–39% in Armenians and Iraqi Jews, to 20% in Turks, North African and Ashkenazi Jews, and Arabs which leads to a significant economic burden [1,2]. The disease is mostly caused by recessively inherited

 doi:10.20944/preprints202403.1184.v1

mutations in *MEFV*, which encodes pyrin protein playing an important role in inflammatory processes [3]. There are two "mutation hot-spots" located in the 2nd (E148Q) and 10th (M694V, M694I, M680I и V726A) exons. These mutations account for over 90% of all FMF cases [4]. Mutated pyrin causes an exaggerated inflammatory response by uncontrolled interleukin-1 (IL-1) secretion [5]. Besides the advances in molecular genetics of FMF, the molecular mechanisms underlying the disease are not fully understood. These questions have been studied using a battery of experimental and *in silico* methods. Thus, molecular dynamic simulations gain insight into the role of mutations on pyrin structure, function, and interactions [6,7]. Another study of polymorphonuclear neutrophils of FMF patients suggests increased sensitivity of mutated pyrin inflammasome towards cytoskeletal modifications in the absence of pathogens [8]. A recent study using different cell types (synovial fibroblasts, monocytes, macrophages) showed that inflammation-related functional assays have an anti-inflammatory effect of miR-197-3p [9]. Various cell-line-based models have been developed for a more comprehensive understanding of the etiology and pathogenesis of FMF [10]. Also, gene editing with CRISPR/Cas9 has been used to understand the effect of the *MEFV* E583A mutation on IL-1β secretion [11]. However, immortalized cell lines have their limitations in mimicking the disease of interest since they do not account for patient genetic variability [12], may accumulate mutations and lack genetic and cellular diversity, and mostly represent cancer-derived cells [13]. On the other side, patient primary cells have limited potential for cultivation and maintenance, posing limitations for experiments.

Induced pluripotent stem cells (iPSCs) are considered a unique tool for studying molecular genetic mechanisms of this disease, disease modeling, and screening of potential drugs [14–16]. The main advantage of iPSCs is the almost unlimited ability of cultivation and differentiation serving as a proper source of pluripotent stem cells and any type of cells in the living organism. IPSCs were successfully used for studying autoinflammatory [17,18], neurodegenerative [17–24], and other diseases. There are few attempts to create iPSCs for FMF patients, for example, a Turkish patient with a homozygous missense mutation (p.Met694Val) in the *MEFV* gene [25].

In this paper, we generated iPSCs from an Armenian FMF patient carrying a homozygous c.2080A>G (M694V) mutation in the *MEFV* gene. Molecular-genetic characterization proved their stemness characteristics. We further differentiated these cells into macrophage-like cells. The morphology analysis showed considerable differences between derived macrophages with mutated *MEFV* gene compared with macrophages derived from iPSCs with wild-type *MEFV* [26].

2. Results

2.1. Generation and Characteristics of iPSCs Associated with the MEFV Gene Mutation

A 20-year-old patient was admitted to the Rheumatology Department of Mikayelyan University Hospital with symptoms relevant to mixed thoracoabdominal form of FMF, pain in joints, arthritis, erysipeloid erythema, and fever. Genetic analysis of the patient revealed pathogenic homozygous missense mutation c.2080A>G (p.M694V, rs61752717) in exon 10 of the *MEFV* gene. We isolated peripheral blood mononuclear cells (PBMCs) in a Ficoll gradient and reprogrammed them using episomal vectors OCT4, KLF4, L-MYC, SOX2, LIN28, and Trp53 [27]. As a result, 10 independent cell lines were obtained, one of which was characterized in detail. All resulting cell lines have a large nuclear-cytoplasmic ratio, grow in densely packed iPSC-like single-layer colonies (Figure 1A), and express the early stem cell marker endogenous alkaline phosphatase (Figure 1B). Cultivation of the resulting cells was carried out on a substrate of mitotically inactivated mouse embryonic fibroblasts (MEF).

 doi:10.20944/preprints202403.1184.v1

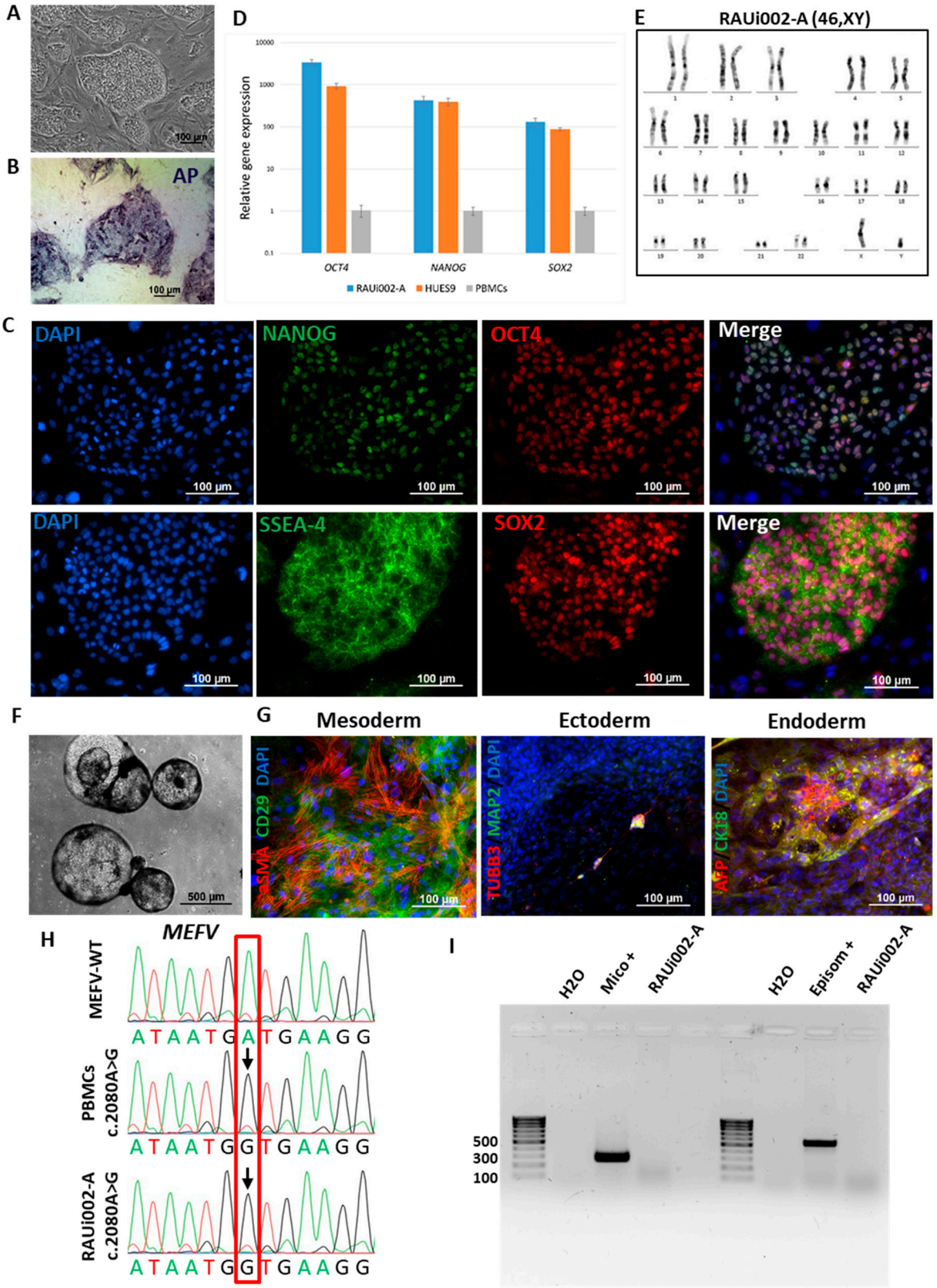

Figure 1. Characteristics of the iPSC cell lines RAUi002-A. (A) Morphology of iPSC colonies. (B) Histochemical detection of alkaline phosphatase (AP). (C) Immunofluorescent staining for pluripotency markers OCT4 (red signal), NANOG (green signal), SSEA-4 (green signal), TRA-1-60 (red signal). (D) Quantitative analysis of the expression of pluripotency markers (OCT4, NANOG, SOX2) using RT-qPCR. Error bars show standard deviation. (E) Karyotype analysis (G-banding) (46,XY). (F) Morphology of embryoid bodies on the 18th day of differentiation. (G)

 doi:10.20944/preprints202403.1184.v1

Immunofluorescent staining for differentiation markers: αSMA (red signal) and CD29 (green signal) (mesoderm); TUBB3/TUJ1 (red signal) and MAP2 (green signal) (ectoderm); AFP (red signal) and CK18 (green signal) (endoderm). Nuclei are stained with DAPI (blue signal). (H) Chromatograms of *MEFV* gene regions of PBMCs of a patient with FMF, and iPSCs with wild-type *MEFV* [26]. The detected polymorphisms are marked with arrows. (I) PCR test for mycoplasma and episomes of the iPSC line (RAUi002-A). Scale bars for (A-C) and (G) - 100 μm. Scale bar for (F) - 500 μm.

One cell line was selected for detailed characterization and was registered in the Human Pluripotent Stem Cell Registry (hPSCreg, https://hpscreg.eu, accessed on 14 March 2024) under the name RAUi002-A. We carried out qualitative (immunofluorescence) and quantitative (RT-qPCR) analyzes of this line for markers of pluripotent cells. Both analyzes demonstrate the presence in cells obtained from a patient with FMF, associated with the genetic variant c.2080A>G (M694V) in the *MEFV* gene, expression of the transcription factors OCT4, SOX2, and NANOG (Figure 1C,D), as well as immunofluorescence showing the expression of surface marker SSEA-4 (Figure 1C). Cytogenetic analysis (G-banding) of the obtained cells showed the presence of a normal karyotype (46,XY) (Figure 1E).

One of the main tests of pluripotency is the ability of cells to give rise to all three germ layers (ectoderm, mesoderm, and endoderm). We performed spontaneous differentiation in embryoid bodies (Figure 1F) and used immunofluorescence analysis of differentiated cells to show the expression of mesoderm markers (α-smooth muscle actin (αSMA) and the surface marker CD29), ectoderm (tubulin β 3 (TUBB3/TUJ1) and mature neural cell markers methionine aminopeptidase 2 (MAP2)), and endoderm (alpha-fetoprotein (AFP) and cytokeratin 18 (CK18)) (Figure 1G). Thus, we have demonstrated that the resulting cells are pluripotent, and we will refer to them as iPSCs.

To confirm the presence of a pathogenic mutation in the resulting iPSC line, Sanger sequencing of DNA isolated from the patient's PBMCs and from the RAUi002-A iPSC line was performed and compared to DNA from a conditionally healthy patient. We found a substitution at position 2080 A to G in exon 10 of the *MEFV* gene in both samples compared to control DNA (Figure 1H, location of substitution indicated by arrow). In addition, to confirm the origin of the iPSCs derived from the patient's PBMCs, STR analysis was performed on the DNA of the PBMC sample and the RAUi002-A line. 25 loci from both samples were analyzed and their identity was shown (data available on request from the authors). This suggests that iPSCs data obtained from an FMF patient can serve as a tool to study the contribution of the p.M694V mutation in the *MEFV* gene to the pathogenesis of FMF disease.

RAUi002-A iPSCs were also analyzed for the presence/absence of residual episomes and culture contamination with mycoplasma. Both PCR analyses showed their complete absence (Figure 1I).

Summary characteristics of the RAUi002-A iPSC line are shown in Table 1.

Table 1. Characteristics and validation of the new line iPSCs RAUi002-A.

Classification	Test	Result	Data
Morphology	Photography Bright field	Normal	Figure 1A
Pluripotency status	Qualitative analysis: Alkaline phosphatase staining	Positive	Figure 1B
	Qualitative analysis: Immunocytochemistry	Positive staining for pluripotency markers: OCT3/4, SOX2, NANOG, SSEA-4	Figure 1C
	Quantitative analysis: RT-qPCR	Expression of pluripotency markers: NANOG, OCT4, SOX2	Figure 1D
Genotype	Karyotype (G-banding)	46,XY	Figure 1E
Mutation analysis	Sanger sequencing of DNA from patient's PBMCs and iPSCs	Homozygous p.M694V (c.2080A>G, rs61752717) in exon 10 of the *MEFV* gene	Figure 1H

 doi:10.20944/preprints202403.1184.v1

Differentiation potential	Embryoid body formation	Positive staining for germ layer markers: αSMA and CD29 (mesoderm); MAP2 and TUBB3/TUJ1 (ectoderm); CK18/AFP (endoderm)	Figure 1G
Specific pathogen-free status	Mycoplasma	Negative	Figure 1I

2.2. Generation and Characteristic of Macrophages from RAUi002-A iPSCs

The resulting iPSC line was specifically differentiated into macrophages to obtain a relevant cell type for further studies on the pathogenesis of FMF. The previously obtained iPSC line K7-4Lf/ICGi022-A was used as a control cell line in the experiment [26]. Differentiation of iPSCs into macrophages was achieved by adding cytokines such as interleukin-3 (IL-3) and macrophage colony-stimulating factor (M-CSF) to the differentiating embryoid bodies (Figure 2A,B) to differentiation along the myeloid pathway and form a homogeneous population of monocytes. As a result, from day 14 of differentiation and over 3 weeks, monocytes were produced in the culture medium that adhered to the plastic and terminally differentiated into macrophage-like cells in the presence of M-CSF. Immunofluorescence for markers specific for mature macrophages, CD14 and CD45, confirmed that the resulting cells were macrophages (Figure 2). IPSC-derived macrophages from a healthy donor were found to have a classic cloaked, spreading morphology (Figure 2C), whereas macrophages with the pathogenic p.M694V mutation in the *MEFV* gene had an elongated morphology with many rounded cells (Figure 2D, middle photo, white arrows).

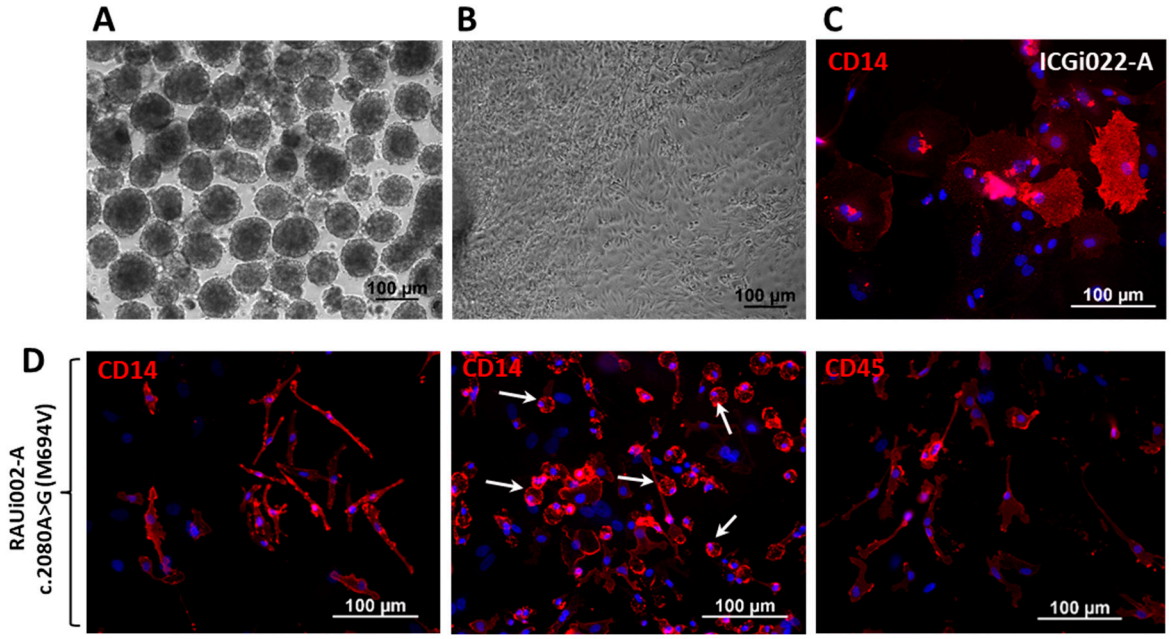

Figure 2. Differentiation of iPSCs into macrophages and characteristics of the resulting cells. (A) Morphology of embryoid bodies on day 4 of differentiation of iPSCs line RAUi002-A. (B) Morphology of spread out embryoid bodies on the 5th day after plating of the RAUi002-A line. (C) Immunofluorescence analysis on macrophage-specific marker CD14 of macrophages derived from control iPSCs line ICGi022-A. (D) Immunofluorescent analysis of macrophage-specific markers CD14 and CD45 of macrophages carrying a mutation c.2080A>G (M694V) in the *MEFV* gene. White arrows indicate rounded cells. Nuclei are stained with DAPI (blue signal). All scale bars: 100 µm.

 doi:10.20944/preprints202403.1184.v1

3. Discussion

In this study, we used the technology of reprogramming PBMCs into a pluripotent state to obtain patient-specific iPSCs from a patient with FMF associated with the pathogenic mutation p.M694V in the *MEFV* gene. The resulting cell line meets all the requirements of pluripotent cells, has a stem cell-like morphology, a normal karyotype, and is capable of producing derivatives of three germ layers. These cells demonstrated their ability to differentiate into macrophages which are one of the key cells involved in the disease pathogenesis [28].

Research related to the establishment of patient-derived iPSCs is expected to be a promising avenue for elucidating the pathogenesis of the diseases, disease therapy, and for drug discovery [29]. They became attractive tools for studying neurodegeneration [21–24,30], cardiac dysfunction [31–33], and genetic disorders, such as Duchenne's muscular dystrophy [34]. Recently these approaches have been actively used for modeling immune-related diseases, such as systemic lupus erythematosus, systemic sclerosis, rheumatoid arthritis, and autoinflammatory syndromes [for review see in 35]. It has been shown that various cell types differentiated from patient-derived iPSCs can be further used for research into the pathogenesis of these diseases.

To our knowledge, a few attempts to generate iPSCs from FMF patients have been made [14,25]. Fidan et al. (2015) reported a cell line derived from fibroblasts of an FMF patient carrying homozygous p.Met694Val mutation in the *MEFV* gene [25]. In our study, we successfully reprogrammed PBMCs of FMF patient with homozygous *MEFV* gene mutation (M694V). This method is less invasive for the patients. Moreover, we performed the differentiation of stem cells into macrophages and analyzed morphological differences between healthy and diseased macrophages. The morphology of macrophage-like cells derived from control iPSCs was significantly different from that of cells derived from iPSCs with a mutation in the *MEFV* gene. Control macrophage-like cells had a flattened morphology, whereas patient-derived cells had an elongated morphology with a large number of rounded, dying cells. We saw that under the same culture conditions, macrophages with a mutation in the *MEFV* gene are less viable, most likely due to a pathogenic mutation. These results are well aligned with the previous observations about the structural and functional features of FMF patients' primary immune cells. Thus, studies indicated characteristics of aged/activated cells (small cell size and granularity, up-regulated CXCR4) for polymorphic neutrophils from the patients in acute flares, while in remission mixed morphology (normal cell size and granularity, up-regulated CD11b, CD49d, CXCR4, and CD62L) has been described [8].

One of the advantages of iPSC-derived macrophages is the preservation of the initial phenotype of the cells. In previous research, it has been shown that iPSC-derived cells at different stages of differentiation demonstrate a complete switch of iPSCs to cells expressing a monocyte, macrophage, or dendritic cell-specific gene profile. Moreover, iPSC-derived LPS-induced macrophages induce the expression of classic macrophage pro-inflammatory response markers [36]. Moreover, the ability to grow an unlimited number of iPSCs and differentiate them into various cells opens multiple avenues for studying FMF pathogenesis, performing drug candidate screening, and developing gene-based therapies. Using patient-specific iPSCs from FMF patients and the CRISPR/Cas9 genome editing system, it will be possible to generate modified isogenic iPSC lines with the corrected mutation in the future. Such cell platforms will be valuable in understanding the effects of the mutations on pyrin inflammasome dysfunction in FMF.

4. Materials and Methods

4.1. Ethics Statement

The study was approved by the Ethics Committee of the Institute of Molecular Biology NAS RA (IRB 00004079, Protocol N3 from 23.08.2021). A patient provided informed consent about the use of the blood sample for planned analysis. ICGi022-A iPSC cell line obtained from a healthy donor [26] was used as a control in the experiments of macrophage differentiation and analysis of the morphological features of mutant and wild-type *MEFV*-carrying cells.

 doi:10.20944/preprints202403.1184.v1

4.2. Detection of MEFV Mutation

Mutations in the *MEFV* gene in the FMF patient was determined by commercially available qPCR assay for 26 most common mutations (FMF Multiplex real-time CPR kit, SNP Biotechnology RnD Ltd, Turkey).

4.3. Reprogramming of PBMCs into iPSCs

PBMCs of a patient with FMF were isolated as described here [22]. iPSCs were obtained by overexpression of reprogramming factors OCT4, KLF4, L-MYC, SOX2, LIN28, and Trp53 using a set of episomal vectors (ID Addgene #41855–58, #41813–14) as previously described [22].

IPSCs were propagated onto feeder layer of mitotically inactivated mouse embryonic fibroblasts (MEF) in iPSC-medium: 82% KnockOut DMEM medium, 15% KoSR, 2 mM Gluta-MAX, 100 U/ml penicillin-streptomycin, 0.1 mM MEM NEAA (all Thermo Fisher Scientific, Waltham, MA, USA), 0.1 mM β-Mercaptoethanol (Sigma-Aldrich, Darmstadt, Germany), 10 ng/ml basic FGF (SCI Store, Moscow, Russia).

IPSCs were passaged using TrypLE Express (Thermo Fisher Scientific, Waltham, MA, USA), splitting 1:10 in the iPSC medium with the addition of 2 μM Thiazovivin (Sigma-Aldrich, Darmstadt, Germany) for the first 24 hours.

4.4. In Vitro Spontaneous Differentiation of RAUi002-A into Three Germ Layers

Differentiation capacity of the iPSCs was estimated by spontaneous differentiation in embryoid bodies as described earlier [37].

4.5. Immunofluorescent Staining of RAUi002-A iPSC Line

For immunofluorescence staining, cells growing on Chambered Coverglass 8-well plates (Thermo Fisher Scientific, Waltham, MA, USA) were fixed with 4% PFA (Sigma-Aldrich, Darmstadt, Germany), permeabilized with 0.5% Triton-X (Thermo Fisher Scientific, Waltham, MA, USA) in PBS for 30 minutes, and incubated in blocking buffer containing 1% BSA (Sigma-Aldrich, Darmstadt, Germany) in PBS at room temperature. Primary antibodies were diluted in a blocking buffer according to Table 2. Cell preparations were incubated with primary antibodies overnight at +4°C. Preparations were washed with PBS twice for 15 min, and secondary antibodies were added for 1.5 hours at room temperature. After incubation, cell preparations were washed twice with PBS and stained with DAPI. Manufacturers, catalog numbers and dilutions of all used antibodies are listed in Table 2. The preparations were analyzed using Nikon Eclipse Ti-E microscope and NIS Elements software.

Table 2. Reagents details.

Antibodies used for immunocytochemistry			
	Antibody	**Dilution**	**Company Cat # and RRID**
Pluripotency Markers	Mouse IgG2b anti-OCT3/4 (C-10)	1:200	Santa Cruz Biotechnology, Dallas, TX, USA, Cat# sc-5279, RRID:AB_628051
	Mouse IgG3 anti-SSEA-4	1:200	Abcam, Cambridge, UK, Cat# ab16287, RRID:AB_778073
	Mouse IgG1 anti-NANOG	1:200	Santa Cruz Biotechnology, Dallas, TX, USA, Cat# sc-293121, RRID:AB_2665475
	Rabbit IgG anti-SOX2	1:500	Cell Signaling, Danvers, MA, USA, Cat# 3579, RRID:AB_2195767
Differentiation Markers	Mouse IgG2a anti- αSMA	1:100	Dako, Glostrup, Denmark, Cat# M0851, RRID:AB_2223500
	Mouse IgG1 anti-CD29 (Integrin beta 1) (TS2/16)	1:100	Thermo Fisher Scientific,Waltham, MA, USA, Cat # 14-0299-82, RRID:AB_1210468

 doi:10.20944/preprints202403.1184.v1

	Mouse IgG2a anti-AFP	1:250	Sigma-Aldrich, Darmstadt, Germany,Cat# A8452, RRID:AB_258392
	Mouse IgG2a anti-Tubulin β 3 (TUBB3)/ Clone: TUJ1	1:1000	BioLegend, San Diego, CA, USA, Cat# 801201, RRID:AB_2313773
	Chicken IgG anti MAP2	1:1000	Abcam, Cambridge, UK, Cat# ab5392, RRID:AB_2138153
	Mouse IgG1 anti-CK18	1:200	Millipore, Burlington, VT, USA Cat# MAB3234, RRID:AB_94763
Macrophage-specific Markers	Mouse IgG2b, κ anti-CD14 APC (Clone MφP9)	1:30	BD Biosciences, Franklin Lakes, NJ, USA, Cat# 345787, RRID:AB_2868813
	Mouse IgG1, κ anti-CD45 PerCP-Cy5.5 CE	1:20	BD Biosciences, Franklin Lakes, NJ, USA, Cat# 332784, RRID:AB_2868632
Secondary antibodies	Goat anti-Mouse IgG3 Cross-Adsorbed Secondary Antibody, Alexa Fluor 488	1:400	Thermo Fisher Scientific,Waltham, MA, USA, Cat# A-21151, RRID:AB_2535784
	Goat anti-Mouse IgG2b Cross-Adsorbed Secondary Antibody, Alexa Fluor 568	1:400	Thermo Fisher Scientific,Waltham, MA, USA, Cat# A-21144, RRID:AB_2535780
	Goat anti-Rabbit IgG (H + L) Alexa Fluor 568	1:400	Thermo Fisher Scientific,Waltham, MA, USA, Cat# A-11011, RRID:AB_143157
	Goat anti-Mouse IgG1 Alexa Fluor 488	1:400	Thermo Fisher Scientific,Waltham, MA, USA, Cat# A-21121, RRID:AB_2535764
	Goat anti-Mouse IgG1 Alexa Fluor 568	1:400	Thermo Fisher Scientific, Waltham, MA, USA, Cat# A21124, RRID:AB_2535766
	Goat anti-Mouse IgG2a Cross-Adsorbed Secondary Antibody, Alexa Fluor 568	1:400	Thermo Fisher Scientific,Waltham, MA, USA, Cat # A-21134, RRID:AB_2535773
	Goat anti-Chicken IgY (H + L) Alexa Fluor 488	1:400	Abcam, Cambridge, UK, Cat # ab150173, RRID:AB_2827653

Primers

	Target	**Size of band**	**Forward/Reverse primer (5′-3′)**
Episomal plasmid vectors detection	EBNA-1	61 bp	TTCCACGAGGGTAGTGAACC/ TCGGGGGTGTTAGAGACAAC
Mycoplasma detection	16S ribosomal RNA gene	280 bp	GGGAGCAAACAGGATTAGATACCCT/ TGCACCATCTGTCACTCTGTTAACCTC
House-keeping gene (RT-qPCR)	beta-2-microglobulin	280 bp	TAGCTGTGCTCGCGCTACT/ TCTCTGCTGGATGACGTGAG
Pluripotency marker (RT-qPCR)	*NANOG*	116 bp	TTTGTGGGCCTGAAGAAAACT/ AGGGCTGTCCTGAATAAGCAG
	OCT4	94 bp	CTTCTGCTTCAGGAGCTTGG/ GAAGGAGAAGCTGGAGCAAA
	SOX2	100 bp	GCTTAGCCTCGTCGATGAAC/ AACCCCAAGATGCACAACTC
Targeted mutation analysis	*MEFV*	297 bp	TGGGATCTGGCTGTCACATTG/ CATTGTTCTGGGCTCTCCGAG

 doi:10.20944/preprints202403.1184.v1

4.6. qPCR Analysis of Expression of Pluripotency Markers in RAUi002-A iPSC Line

For RNA isolation, 2*10^6 cells were lysed in 1 ml TRIzol reagent (Ambion by Life technologies, Carlsbad CA, USA), and processed according to the manufacturer's protocols. The cDNA was synthesized by reverse transcription of 1 μg RNA using M-MuLV reverse transcriptase (Biolabmix, Novosibirsk, Russia).

Quantitative PCR (qPCR) was performed on a LightCycler 480 II system (Roche, Basel, Switzerland) using BioMaster HS-qPCR SYBR Blue 2 × (Biolabmix, Novosibirsk, Russia) with the following program: 95 °C 5 min; 40 cycles: 95 °C 10 s, 60 °C 1 min. The primers used are listed in Table 2. qPCR reactions for each sample were run in triplicate. CT values of the samples for *NANOG*, *OCT4*, and *SOX2* expression were normalized to beta-2-microglobulin (*B2M*), and the results were processed using the ΔΔCT method.

4.7. Karyotyping of RAUi002-A iPSC Line

Karyotype analysis was performed as described earlier [22]. For chromosome banding, samples were stained with DAPI (4,6-diamino-2-phenylindole) solution (200 ng/mL, in 2xSSC) for 5 minutes, rinsed in 2xSSC buffer and water. Air-dried slides were covered with 7-10 μL antifade (Vector, United States) under a coverslip. Analysis of preparations was performed using an Axioplan 2 microscope (Zeiss, Germany) equipped with a CV-M300 CCD camera (JAI Corp., Japan) at the Center for Collective Use of Microscopic Analysis of Biological Objects at the Institute of Cytology and Genetics, Siberian Branch of the Russian Academy of Sciences. ISIS 5 software (MetaSystems Group, Inc., United States) was used for metaphase processing and chromosome folding.

4.8. Genotyping of RAUi002-A iPSC Line

Sanger sequencing was used to confirm the mutation in the *MEFV* gene in the RAUi002-A iPSC line. To confirm the absence of *MEFV* mutations, Sanger sequencing was performed also for the line K7-4Lf/ICGi022-A used as a control sample. The list of primers used is shown in Table 2. Genome DNA was isolated using Quick-DNA Miniprep Kit (Zymo Research, Irvine, CA, USA). PCR reactions were run on a T100 thermal cycler (Bio-Rad) using BioMaster HS-Taq PCR-Color (2×) (Biolabmix, Novosibirsk, Russia) with the program: 95 ◦C, 3 min; further 35 cycles: 95 ◦C, 30 s; 60 ◦C, 30 s; 72 ◦C, 30 s; and 72 ◦C, 5 min. For Sanger sequencing, we used BigDye Terminator V. 3.1. Cycle Sequencing Kit (Applied Biosystems, Austin, TX, USA). Sequencing reactions were analyzed on an ABI 3130XL genetic analyzer at the Genomics Center of the SB RAS (http://www.niboch.nsc.ru/doku.php/corefacility, accessed on 14 March 2024).

STR profiling was performed using AmpFlSTR Identifiler (Applied Biosystems) and Investigator HDplex (QIAGEN) by Genoanalytica company (https://www.genoanalytica.ru, accessed on 14 March 2024).

4.9. Detection of Mycoplasma and Reprogramming Vectors in RAUi002-A iPSC Line

The presence of episomal reprogramming vectors and mycoplasma contamination was assessed by PCR (95°C, 5 min; 35 cycles: 95°C, 15 s, 62°C, 15 s, 72°C, 20 s) using primers listed in Table 2 [27,38].

4.10. Differentiation of RAUi002-A iPSC Line into Macrophages

Differentiation of iPSCs into macrophages was performed according to a previously published protocol [39] with modifications. IPSCs were placed on a Petri dish (D60 mm) coated with mitotically inactivated MEFs. Dense iPSC colonies were detached with 0.15% collagenase type IV (Thermo Fisher Scientific, Waltham, MA, USA), washed with medium, and transferred to a Petri dish (D60 mm) coated with 1% agarose (Sigma-Aldrich, Darmstadt, Germany) in iPSC medium without the addition of bFGF. On day 4 of culture, the formed embryoid bodies were transferred to 3 wells of a 6-well plate coated with 0.1% gelatin (Sigma-Aldrich, Darmstadt, Germany) for spreading and differentiation into monocyte-like cells in RPMI medium supplemented with 10% fetal bovine serum, 2 mM GlutaMax, 100 U/ml penicillin-streptomycin, 0. 1 mM MEM NEAA, 1 mM sodium pyruvate (all Thermo Fisher

 doi:10.20944/preprints202403.1184.v1

Scientific, Waltham, MA, USA), 0.1 mM 2-mercaptoethanol (2-mce, Sigma-Aldrich, Darmstadt, Germany), 25 ng/ml IL-3 and 100 ng/ml M-CSF (both SCI Store, Moscow, Russia). From day 14-19 of culture, the cell suspension was collected from embryoid bodies containing monocyte-like cells, centrifuged at 300 g for 5 min, and seeded onto Chambered Coverglass 8-well plates pretreated with 0.1% gelatin for immunofluorescence staining.

Author Contributions: Conceptualization, S.M.Z., R.Z., A.A. and V.S.V.; methodology, E.V.G.; validation, E.V.G. and S.P.M.; formal analysis, A.A.M.; investigation, E.V.G., J.M.M., S.P.M., L.V.K., V.H.H.; resources, S.M.Z.; data curation, R.Z., A.A., S.M.Z. and E.V.G.; interpretation of data, S.M.Z., R.Z., A.A., V.S.V.; writing—original draft preparation, E.V.G. and A.A.M.; writing—review and editing, R.Z. and A.A.; visualization, E.V.G., R.Z. and A.A.; supervision, S.M.Z., R.Z. and A.A.; project administration, R.Z. and A.A.; funding acquisition, S.M.Z. and R.Z. All authors have read and agreed to the published version of the manuscript.

Funding: The cell reprogramming and characterization was funded by the Ministry of Science and Higher Education of the Russian Federation, Agreement No. 075-15-2021-1063 of 09/28/2021. PBMCs isolation and molecular-genetic characterisation work was supported by the Higher Science and Education Committee of the Ministry of Health RA, in the frames of the research project N 21SCG-1F010 and research grant provided by the Armenian Engineers and Scientists of America (PI: Dr. Roksana Zakharyan). The immunofluorescent imaging was performed using resources of the Common Facilities Center of Microscopic Analysis of Biological Objects, ICG SB RAS (https://ckp.icgen.ru/ckpmabo/, accessed on 14 March 2024), supported by the Budget project of the Institute of Cytology and Genetics (FWNR-2022-0015).

Institutional Review Board Statement: The study was conducted in accordance with the Declaration of Helsinki and approved by the Ethics Committee of the Institute of Molecular Biology NAS RA (IRB 00004079, Protocol N3 from 23.08.2021).

Informed Consent Statement: Informed consent was obtained from all subjects involved in the study.

Data Availability Statement: The data presented in this study are openly available in the Human Pluripotent Stem Cell Registry (https://hpscreg.eu/cell-line/RAUi002-A and https://hpscreg.eu/cell-line/ICGi022-A, all accessed on 14 March 2024).

Acknowledgments: The equipment of the Meshalkin National Medical Research Center, Ministry of Health of the Russian Federation (Novosibirsk, Russia) was used for routine cell imaging.

Conflicts of Interest: The authors declare no conflicts of interest.

References

1. Chae, J.J.; Aksentijevich, I.; Kastner, D.L. Advances in the understanding of familial Mediterranean fever and possibilities for targeted therapy. *Br J Haematol*. **2009**, *146*, 467-478.
2. Booty, M.G.; Chae, J.J.; Masters, S.L.; Remmers, E.F.; Barham, B.; Le, J.M.; Barron, K.S.; Holland, S.M.; Kastner, D.L.; Aksentijevich, I. Familial Mediterranean fever with a single MEFV mutation: where is the second hit? *Arthritis Rheum.* **2009**, *60*, 1851-1861. https://doi.org/10.1002/art.24569.
3. Cantarini, L.; Rigante, D.; Brizi, M.G.; Lucherini, O.M.; Sebastiani, G.D.; Vitale, A.; Gianneramo, V.; Galeazzi, M. Clinical and biochemical landmarks in systemic autoinflammatory diseases. *Ann Med*. **2012**, *44*, 664-673. https://doi.org/10.3109/07853890.2011.598546.
4. French FMF Consortium. A candidate gene for familial Mediterranean fever. *Nat Genet*. **1997**, *17*, 25-31. https://doi.org/10.1038/ng0997-25.
5. Özen, S.; Batu, E.D.; Demir, S. Familial Mediterranean Fever: recent developments in pathogenesis and new recommendations for management. *Front. Immunol.* **2017**, *8*, 253. https://doi.org/10.3389/fimmu.2017.00253
6. Sargsyan, A.; Sahakyan, H.; Nazaryan, K. Effect of colchicine binding site inhibitors on the tubulin intersubunit interaction. *ACS Omega* **2023**, *8*, 29448-29454. https://doi.org/10.1021/acsomega.3c02979.
7. Arakelov, G.; Arakelov, V.; Nazaryan, K. Complex formation dynamics of native and mutated pyrin's B30.2 domain with caspase-1. *Proteins* **2018**, *86*, 676-683. https://doi.org/10.1002/prot.25494.
8. Martirosyan, A.; Poghosyan, D.; Ghonyan, S.; Mkrtchyan, N.; Amaryan, G.; Manukyan, G. Transmigration of neutrophils from patients with Familial Mediterranean fever causes increased cell activation. *Front. Immunol.* **2021**, *12*, 672728. https://doi.org/10.3389/fimmu.2021.672728.
9. Akkaya-Ulum, Y.Z.; Akbaba, T.H.; Tavukcuoglu, Z.; Chae, J.J.; Yilmaz, E.; Ozen, S.; Balci-Peynircioglu, B. Familial Mediterranean fever-related miR-197-3p targets IL1R1 gene and modulates inflammation in monocytes and synovial fibroblasts. *Sci. Rep.* **2021**, *11*, 685. https://doi.org/10.1038/s41598-020-80097-4.

10. Mezher, N.; Mroweh, O.; Karam, L.; Ibrahim, J.N.; Kobeissy, P.H. Experimental models in Familial Mediterranean Fever (FMF): Insights into pathophysiology and therapeutic strategies. *Exp. Mol. Pathol.* **2024**, *135*, 104883.
11. Wang, Q.; Jin, T.; Jian, Sh.; Han, X.; Song, H.; Zhou, Q.; Yu, X. A dominant pathogenic MEFV mutation causes atypical pyrin-associated periodic syndromes. *JCI Insight.* **2023**, *8*, e172975. https://doi.org/10.1172/jci.insight.172975.
12. Volpato, V.; Webber, C. Addressing variability in iPSC-derived models of human disease: guidelines to promote reproducibility. *Dis. Model. Mech.* 2020, 13, dmm042317. https://doi.org/10.1242/dmm.042317.
13. Gorringe, K.L.; Chin, S.F.; Pharoah, P.; Staines, J.M.; Oliveira, C.; Edwards, P.A.W.; Caldas, C. Evidence that both genetic instability and selection contribute to the accumulation of chromosome alterations in cancer. *Carcinogenesis* **2005**, *26*, 923–930. https://doi.org/10.1093/carcin/bgi032
14. Shiba, T.; Tanaka, T.; Ida, H.; Watanabe, M.; Nakaseko, H.; Osawa, M.; Shibata, H.; Izawa, K.; Yasumi, T.; Kawasaki, Y.; Saito, M.K.; Takita, J.; Heike, T.; Nishikomori, R. Functional evaluation of the pathological significance of MEFV variants using induced pluripotent stem cell-derived macrophages. *J. Allergy Clin. Immunol.* **2019**, *144*, 1438-1441.e12. https://doi.org/10.1016/j.jaci.2019.07.039.
15. Saito, M.K. Elucidation of the pathogenesis of autoinflammatory diseases using iPS cells. *Children (Basel)* **2021**, *8*, 94. https://doi.org/10.3390/children8020094.
16. Rowe, R.G. & Daley, G.Q. Induced pluripotent stem cells in disease modelling and drug discovery. *Nat. Rev. Genet.* **2019**, *20*, 377-388. https://doi.org/10.1038/s41576-019-0100-z.
17. Hew, M.; O'Connor, K.; Edel, M.J.; Lucas, M. The possible future roles for iPSC-derived therapy for autoimmune diseases. *J. Clin. Med.* **2015**, *4*, 1193-1206. https://doi.org/10.3390/jcm4061193.
18. Tanaka, T.; Shiba, T.; Honda, Y.; Izawa, K.; Yasumi, T.; Saito, M.K.; Nishikomori R. Induced pluripotent stem cell-derived monocytes/macrophages in autoinflammatory diseases. *Front. Immunol.* **2022**, *13*, 870535. https://doi.org/10.3389/fimmu.2022.870535.
19. Okano, H. & Morimoto, S. iPSC-based disease modeling and drug discovery in cardinal neurodegenerative disorders. *Cell Stem Cell* **2022**, *29*, 189-208. https://doi.org/10.1016/j.stem.2022.01.007.
20. Pandey, Sh.; Jirásko, M.; Lochman, J.; Chvátal, A.; Dvorakova, M.C.; Kučera, R. iPSCs in neurodegenerative disorders: a unique platform for clinical research and personalized medicine. *J. Pers. Med.* **2022**, *12*, 1485. https://doi.org/10.3390/jpm12091485
21. Grigor'eva, E.V.; Malankhanova, T.B.; Surumbayeva, A.; Pavlova, S.V.; Minina, J.M.; Kizilova, E.A.; Suldina, L.A.; Morozova, K.N.; Kiseleva, E.; Sorokoumov, E.D.; et al. Generation of GABAergic striatal neurons by a novel iPSC differentiation protocol enabling scalability and cryopreservation of progenitor cells. Cytotechnology. **2020**, *72*, 649–663.. https://doi.org/10.1007/s10616-020-00406-7
22. Grigor'eva, E.V.; Kopytova, A.E.; Yarkova, E.S.; Pavlova, S.V.; Sorogina, D.A.; Malakhova, A.A.; Malankhanova, T.B.; Baydakova, G.V.; Zakharova, E.Y.; Medvedev, S.P.; Pchelina, S.N.; et al. Biochemical Characteristics of iPSC-Derived Dopaminergic Neurons from N370S GBA Variant Carriers with and without Parkinson's Disease. Int. J. Mol. Sci. 2023a, 24, 4437. https://doi.org/10.3390/IJMS24054437.
23. Malankhanova, T.B.; Suldina, L.A.; Grigor'eva, E.V.; Medvedev, S.P.; Minina, J.M.; Morozova, K.N.; Kiseleva, E.; Zakian, S.M.; Malakhova, A.A. A human induced pluripotent stem cell–derived isogenic model of Huntington's disease based on neuronal cells has several relevant phenotypic abnormalities. J. Pers. Med. **2020**, *10*, 215. https://doi.org/10.3390/ijms24054437
24. Ustyantseva, E.; Pavlova, S.V.; Malakhova, A.A.; Ustyantsev, K.; Zakian, S.M.; Medvedev, S.P. Oxidative stress monitoring in iPSC-derived motor neurons using genetically encoded biosensors of H2O2. Sci Rep. **2022**, *12*, 8928. https://doi.org/10.1038/s41598-022-12807-z
25. Fidan, K.; Kavaklıoğlu, G.; Ebrahimi, A.; Özlü, C.; Ay, N.Z.; Ruacan, A.; Gül, A.; Önder, T.T. Generation of integration-free induced pluripotent stem cells from a patient with Familial Mediterranean Fever (FMF). *Stem Cell Res.* **2015**, *15*, 694-696. https://doi.org/10.1016/j.scr.2015.10.018.
26. Malakhova, A.A.; Grigor'eva, E. V.; Pavlova, S. V.; Malankhanova, T.B.; Valetdinova, K.R.; Vyatkin, Y. V.; Khabarova, E.A.; Rzaev, J.A.; Zakian, S.M.; Medvedev, S.P. Generation of induced pluripotent stem cell lines ICGi021-A and ICGi022-A from peripheral blood mononuclear cells of two healthy individuals from Siberian population. *Stem Cell Res.* 2020, 48. https://doi.org/10.1016/j.scr.2020.101952.
27. Okita, K.; Yamakawa, T.; Matsumura, Y.; Sato, Y.; Amano, N.; Watanabe, A.; Goshima, N.; Yamanaka, S. An efficient nonviral method to generate integration-free human-induced pluripotent stem cells from cord blood and peripheral blood cells. *Stem Cells*. **2013**, *31*, 458-466. https://doi.org/10.1002/stem.1293.
28. Savran, Y.; Sari, I.; Kozaci, D.L.; Gunay, N.; Onen, F.; Akar, S. Increased levels of macrophage migration inhibitory factor in patients with Familial Mediterranean Fever. *Int. J. Med. Sci.* **2013**, *10*, 836-839. https://doi.org/10.7150/ijms.6116.
29. Nicholson, M.W.; Ting, Ch.Y.; Chan, D.Z.H.; Cheng, Yu.; Lee, Yu; Hsu, C.; Huang, C.; Hsieh P.C.H. Utility of iPSC-derived cells for disease modeling, drug development, and cell therapy. *Cells* **2022**, *11*, 1853. https://doi.org/10.3390/cells11111853.

30. Chamberlain, S.J. Disease modelling using human iPSCs. *Hum. Mol. Genet.* 2016, 25(R2), R173-R181. https://doi.org/10.1093/hmg/ddw209.
31. Csöbönyeiová, M.; Polák, S.; Danišovič, L. Perspectives of induced pluripotent stem cells for cardiovascular system regeneration. *Exp. Biol. Med (Maywood).* **2015**, *240*, 549-556. https://doi.org/10.1177/1535370214565976.
32. Rikhtegar, R.; Pezeshkian, M.; Dolati, S.; Safaie, N.; Rad, A.A.; Mahdipour, M.; Nouri, M.; Jodati, A.R.; Yousefi, M. Stem cells as therapy for heart disease: iPSCs, ESCs, CSCs, and skeletal myoblasts. *Biomed. Pharmacother.* **2019**, *109*, 304-313. https://doi.org/10.1016/j.biopha.2018.10.065.
33. Parrotta, E.I.; Lucchino, V.; Scaramuzzino, L.; Scalise, S.; Cuda, G. Modeling cardiac disease mechanisms using induced pluripotent stem cell-derived cardiomyocytes: progress, promises and challenges. *Int. J. Mol. Sci.* **2020**, *21*, 4354. https://doi.org/10.3390/ijms21124354.
34. Danisovic, L.; Culenova, M.; Csobonyeiova, M. Induced pluripotent stem cells for Duchenne muscular dystrophy modeling and therapy. *Cells* **2018**, *7*, 253. https://doi.org/10.3390/cells7120253.
35. Shoda, H.; Natsumoto, B.; Fujio, K. Investigation of immune-related diseases using patient-derived induced pluripotent stem cells. Inflamm. *Regen.* **2023**, *43*, 51. https://doi.org/10.1186/s41232-023-00303-4.
36. Monkley, S.; Krishnaswamy, J.K.; Göransson, M.; Clausen, M.; Meuller, J.; Thörn, K.; Hicks, R.; Delaney, S.; Stjernborg, L. Optimised generation of iPSC-derived macrophages and dendritic cells that are functionally and transcriptionally similar to their primary counterparts. *PLoS One* **2020**, *15*, e0243807. https://doi.org/10.1371/journal.pone.0243807.
37. Grigor'eva, E.V.; Malakhova, A.A.; Ghukasyan, L.; Hayrapetyan, V.; Atshemyan, S.; Vardanyan, V.; Zakian, S.M.; Zakharyan, R.; Arakelyan, A. Generation of three induced pluripotent stem cell lines (RAUi001-A, RAUi001-B and RAUi001-C) from peripheral blood mononuclear cells of a healthy Armenian individual. Stem Cell Research. 2023b, 71, 103147. https://doi.org/10.1016/j.scr.2023.103147.
38. Choppa, P.C.; Vojdani, A.; Tagle, C.; Andrin, R.; Magtoto, L. Multiplex PCR for the detection of mycoplasma fermentans, M. hominis and M. penetrans in cell cultures and blood samples of patients with chronic fatigue syndrome. *Mol. Cell. Probes.* **1998**, *12*, 301–308. https://doi.org/10.1006/mcpr.1998.0186.
39. Wilgenburg, B.; Browne, C.; Vowles, J.; Cowley, S.A. Efficient, long term production of monocyte-derived macrophages from human pluripotent stem cells under partly-defined and fully-defined conditions. *PLoS One.* **2013**, *8*, e71098. https://doi.org/10.1371/journal.pone.0071098